AC Loss Characteristics of the KSTAR CSMC Estimated by Pulse Test

S. Lee, Y. Chu, W. H. Chung, S. J. Lee, S. M. Choi, S. H. Park, H. Yonekawa, S. H. Baek, J. S. Kim, K. W. Cho, K. R. Park, B. S. Lim, Y. K. Oh, K. Kim, J. S. Bak, and G. S. Lee

***Abstract*—The KSTAR Central Solenoid Model Coils (CSMC), which are in the form of split coils with same dimension, have been tested. The CSMC were successfully charged up to 20 kA and down to zero with different ramp rates. Various pulse waveforms were applied to the CSMC to analyse the AC-loss characteristics of the coils. The measurement method was a gas-flow calorimetry. In this work, two types of waveforms, the DC-biased sinusoidal wave ($I_{dc} = 2, 4$ kA; $\Delta I_{ac} = 1$ kA; $f = 0.08 \sim 0.67$ Hz) and a single triangular pulse ($I_{max} = 6 \sim 10$ kA; $dI/dt = 0.5 \sim 2$ kA/s), are selected and analysed. From the measured data at the one outlet where helium channel 3 and 4 are merged, the AC loss parameters, related with the hysteresis loss and the coupling loss, are calculated. The B-field strength differs depending on the position within the cooling channels. The spatial field variation and the ramp rate were 0.048∼1.9 T and 8.1∼ 71 mT/s for the DC-biased sinusoidal waves, while 0.29∼ 4.3 T and 0.024∼ 0.86 T/s for the triangular pulses. The measured AC losses are compared with estimated values and the behavior agrees well. The coupling time constant ($n\tau$) varies with the field strength. In case of the triangular pulses, $n\tau$ increases by increasing the field amplitude and the maximum value of $n\tau$ is 41 ms with $I_{max} = 10$ kA.**

***Index Terms*—AC loss, coupling time constant, CS model coil, KSTAR.**

I. Introduction

THE KSTAR device is an experimental tokamak using all superconducting magnets to make long pulse operation possible. All magnets are wound using CICCs (Cable-In-Conduit Conductor) with a continuous winding scheme to remove internal joints [1]. The KSTAR TF (Toroidal Field) magnet system consists of 16 D-shape coils, which are made of Nb_3Sn strand with Incoloy 908 jacket. The PF (Poloidal Field) magnet system is composed of 8 CS (Central Solenoid) coils (PF1-4UL) and 6 outer PF coils (PF5-7UL). Nb_3Sn Incoloy 908 CICC is also used for these coils except for PF6-7UL, which are made of NbTi stainless steel 316LN CICC.

According to the reference operation scenario of the KSTAR device, the maximum magnetic field strength is 8 T and the maximum ramp rate is 12 T/s. A background-field magnet system has been developed to simulate the environment for the KSTAR conductor tests [2]. The main coils of the system are able to provide ±8 T at the center of the magnet bore. In order to validate the design of the KSTAR CS coils, it was constructed using the KSTAR CS CICC. Therefore, it serves as a KSTAR Central Solenoid Model Coil (CSMC). The major parameters of the CSMC are shown in Table I. The tube-mill process is adopted for the jacketing of CICC [3], [4].

TABLE I
MAJOR PARAMETERS OF THE KSTAR CS MODEL COIL

Strand	
Superconductor	Nb_3Sn
Strand diameter	0.78 mm after chrome plating
Cu/non-Cu ratio	1.5
Jc (4.2 K, 12 T, 0.1 V/cm)	> 750 mm^2
Hysteresis loss (±3 T, 4.2 K)	< 250 mJ/cc-nonCu
n-value	> 20
RRR	> 100
Conductor	
Conduit material	Incoloy 908
Void fraction	36.3%
Number of strands	360 (SC 240, Cu 120)
Cabling pattern	3x4x5x6
Cable twist pitch	40, 80, 145, 237 mm
Conduit dimension	w22.3, h22.3, t2.41 mm
Coil	
Number of coils	2
Inner diameter	740 mm
Outer diameter	1488 mm
Thickness	398 mm
Number of turns per coil	240 (15 x 16 pk)
Inductance	134.4 mH
Stored energy	34.3 MJ @22.6 kA

II. Experimental Setup and Measurement Method

The CSMC is composed of two split solenoids (MC1, MC2) with the same dimension and is installed in the large vacuum cryostat for test as shown in Fig. 1. There are eight cooling channels for each coil. One channel is 105 m long and covers two layers of the coil. The MC1 and the MC2 are connected in series.

Manuscript received September 19, 2005. This work was supported by the Korean Ministry of Science and Technology under the KSTAR project.

S. Lee is with the Korea Basic Science Institute, Daejeon, 305-380, Korea and also with the Department of Nuclear and Quantum Engineering in KAIST, Daejeon 305-701, Korea (e-mail: silee@kbsi.re.kr).

Y. Chu, S. J. Lee, S. H. Park, H. Yonekawa, S. H. Baek, J. S. Kim, K. W. Cho, K. R. Park, B. S. Lim, Y. K. Oh, K. Kim, J. S. Bak, and G. S. Lee are with the Korea Basic Science Institute, Daejeon, 305-380, Korea.

W. H. Chung is with the Korea Basic Science Institute, Daejeon, 305-380, Korea and also with the Department of Mechanical Engineering in KAIST, Daejeon 305-701, Korea.

S. M. Choi is with the Department of Nuclear and Quantum Engineering in KAIST, Daejeon 305-701, Korea.

Digital Object Identifier 10.1109/TASC.2006.870541

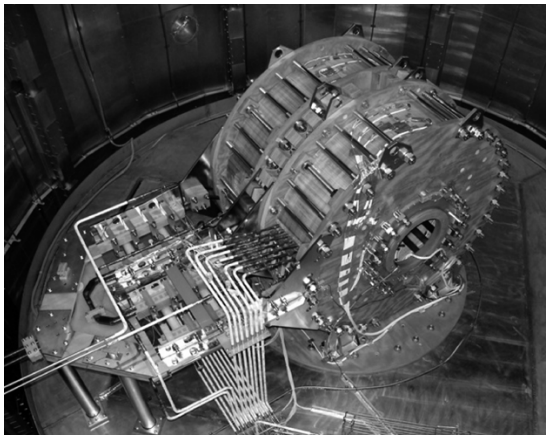

Fig. 1. KSTAR CSMC installed inside the large vacuum cryostat. The coil system consists of two split coils, MC1 (right side) and MC2 (left side).

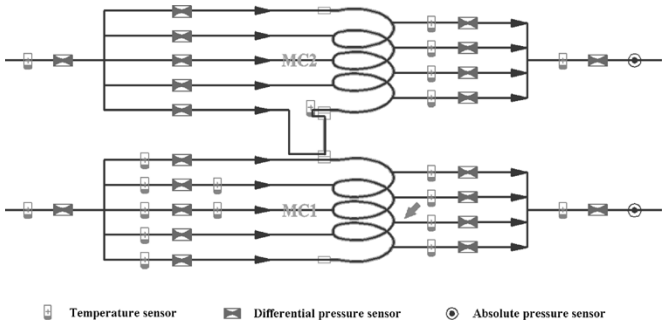

Fig. 2. Calorimetric measurement system arrangement diagram: An arrow points the 112R line, which is used for analysis.

AC losses of the coil are measured by a gas-flow calorimetry and mass flow meters, temperature sensors, and pressure sensors are installed on the helium lines as shown in Fig. 2. For the AC loss analysis, the cooling channels not linked with joints are preferable since there is no joule loss of joints and it is more relevant to the AC loss measurement of the conductor. The channels linked to the return line 2 (112R) of the MC1 are analysed.

AC losses of a CICC can be expressed by the following equation [5].

$$Q_{\text{channel}} = \int \dot{m}\,\{h(T,P) - h_0\}\,dt \tag{1}$$

where $\dot{m}$ is the mass-flow rate at the outlet (g/s), $h(T,P)$, enthalpy at outlet (J/g), and h_0, initial enthalpy at outlet (J/g).

Because of the schematic of the continuous winding method, helium flow at an inlet feed-through is bifurcated into two adjacent outlet feed-throughs. Since helium flows from two inlets are mixed at one outlet, the measured loss is the sum of those from two adjacent channels. The measured AC loss on the line 112R corresponds to the heat generated through both the channel 3 (Ch3) and channel 4 (Ch4).

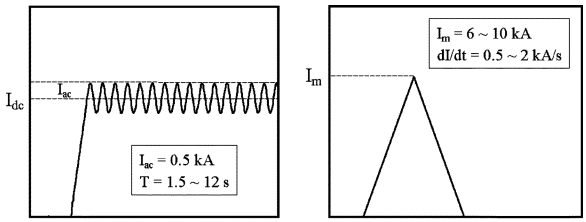

Fig. 3. Pulses for the AC loss analysis: Discrete values for T and dI/dt were used for the measurement. (a) DC-biased sine pulse; (b) singular triangular pulse.

III. Analysis Method

In order to estimate the AC performance of the CSMC, two kinds of waveforms are selected and analysed. One is a sinusoidal wave with DC offset, and the other is a single triangular pulse. The frequency of the sine wave and the ramping rate of the triangular pulse are as shown in Fig. 3. In case of the DC-biased sine wave, in order to extract the effect of the sinusoidal ripple, the AC loss during the trapezoidal pulse is measured and the loss is subtracted from the total AC loss.

Since the applied current in this study is much less than the critical current of the CSMC (less than 10% of the critical current), transport current loss can be neglected [6] and only the hysteresis loss and the coupling current loss are considered.

A. Hysteresis Loss

For the pulses described above, hysteresis loss can be estimated using the following equations [7].

1) DC Biased Sine Wave: $b(t) = b_{dc} + b_{ac}\sin(\omega t)$*:*

$$Q_h = \frac{\Delta B_{ac}^2}{2\mu_0}\left[\frac{4}{3}\frac{\Delta B_{\text{ac}}}{\Delta B_p(B_{\text{dc}})} - \frac{2}{3}\left(\frac{\Delta B_{\text{ac}}}{\Delta B_p(B_{\text{dc}})}\right)^2\right] \quad \Delta B_{\text{ac}} \le \Delta B_p(B_{\text{dc}}) \tag{2}$$

$$Q_h = \frac{2\Delta B_p^2(B_{\text{dc}})}{3\mu_0}\left[\frac{\Delta B_{\text{ac}}}{\Delta B_p(B_{\text{dc}})} - \frac{1}{2}\right] \quad \Delta B_{\text{ac}} > \Delta B_p(B_{\text{dc}}) \tag{3}$$

and

$$\Delta B_p(B_{dc}) = \frac{2}{\pi}\mu_0 J_{c,SC}(B_{\text{dc}}) D_{\text{eff}} \tag{4}$$

where, $\Delta B_{\text{ac}} = 2B_{ac}$, D_{eff} is an effective filament diameter, and the unit of Q_h is J/m^3-superconductor.

2) Triangular Pulse:

$$Q_h \approx \frac{4}{3\pi} D_{\text{eff}} \int_{B_{\min}}^{B_{\max}} J_{c,SC}(B)dB \left[\text{J}/\text{m}^3 - \text{nonCu}\right]. \tag{5}$$

For the calculation, D_{eff} is assumed to be about 13 μm, which corresponds to the Q_h of 250 mJ/cc, being the requirement of the KSTAR HP-III strand. $J_{c,SC}(B_{dc})$ was calculated using Ekin-Summer's scaling law.

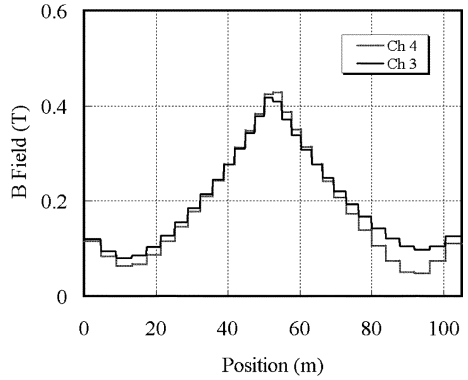

Fig. 4. Magnetic field profile along Ch3 and Ch4 of MC1 which was used for the AC characteristic analysis of the KSTAR CSMC: $\mathrm{I_{op}} = 1\,\mathrm{kA}$.

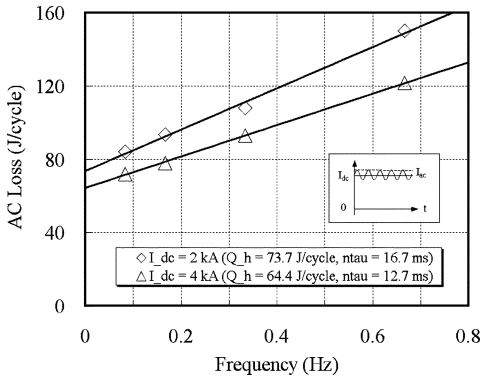

Fig. 5. Frequency spectrum of the total measured AC loss in case of the DC-biased sine wave application: $\mathrm{I_{ac}} = 0.5\,\mathrm{kA}$.

TABLE II
DISTRIBUTION OF THE MAGNETIC FIELD AMPLITUDE FOR THE DC-BIASED SINUSOIDAL WAVE AND THE TRIANGULAR PULSE

I [kA]	Min [T]	Max [T]	Avg [T]
2	0.048	1.1	0.47
4	0.14	1.9	0.84
6	0.29	2.6	1.1
7	0.34	3.0	1.3
8	0.39	3.4	1.5
9	0.43	3.9	1.7
10	0.48	4.3	1.9

B. Coupling Current Loss

1) DC Biased Sine Wave: When the ripple-field effect is considered only, the coupling loss is expressed as follows [8].

$$Q_c = \frac{\pi \Delta B_{\mathrm{ac}}^2 \omega n \tau}{4\mu_0(1+\omega^2\tau^2)}\ [\mathrm{J/cycle/m^3}] \tag{6}$$

where τ is the coupling current time constant of the cable, and the superconductor geometry factor $n = 2$ in our case.

2) Triangular Pulse:

$$Q_c = \frac{2B_m^2 n\tau}{\mu_0 t_m}\ [\mathrm{J/m^3}] \tag{7}$$

where B_m is the maximum field and t_m is the time at the maximum field.

In the coupling loss calculation, the volume of the SC strands and the segregated copper strands is taken into account. The volume increment during cabling is also considered. On the other hand, the hysteresis loss calculation includes only the non-copper volume with its cabling effect.

The field distribution along the channels is calculated and the magnetic field profiles of the Ch3 and Ch4 are shown in Fig. 4. The spatial variation of the field amplitude is shown in Table II for the two types of waveforms. The ramp rates are 8.1∼71 mT/s for the DC-biased sinusoidal waves and 0.024∼0.86 T/s for the triangular pulses, being in the range comparable to the condition of the ITER CSMC test [9].

IV. RESULTS AND DISCUSSION

During the test, the temperature and the mass-flow rate at both the inlet and the outlet was not kept constant, especially when the AC loss was changing rapidly. And also the cooling power varied adaptively and this adaptive power loss or gain had to be considered. Therefore, power variation at the inlet is integrated and subtracted from Q_{channel} in (1). The measured data on the return line 112R is analysed. In the estimation of the hysteresis loss, the temperature and the total longitudinal strain are set to 5 K and -0.3%, respectively.

Fig. 5 shows the measurement results for the DC-biased sine waves. Two levels of bias current were applied, 2 and 4 kA. The amplitude and the frequency range of the sine wave were 0.5 kA and 0.08∼0.67 Hz, respectively. The shot duration was more than 12 minutes.

The coupling loss shows a linear dependence on the frequency of the sine wave. This result tells us the existence of substantial cyclic-loading effects [10]. In fact, the coil was charged up to 20 kA with more than 20 times before this waveform was applied. The BI load at 20 kA along the corresponding channels has the distribution of 1.8∼9.8 MPa and the average is 4.3 MPa. In this level of stress, it was reported that the coupling loss of the coil would be decreased cycle by cycle [11]. From this point of view, the coil has been stabilized during the previous excitation.

The coupling time constant $(n\tau)$ of the 4-kA case was measured to be 31% less than that of the 2-kA case. Referring (6) with $\omega\tau \ll 1$, the coupling loss is proportional to the square of the applied AC field (B_{ac}^2) and the DC bias field does not affect the result. Since the average B_{ac}^2 is same both for the 2-kA case and the 4-kA case, the coupling losses of both cases are expected be the same. However, the result is contradictory to this fact and it should be further investigated.

Hysteresis loss is estimated to be 67.5 J/cycle in the 2-kA case and 55.9 J/cycle of the 4-kA case. The error between the measured data and the estimated value is 9% and 15% for the 2-kA case and the 4-kA case, respectively. The measured hysteresis loss of the 2-kA case is larger than that of the 4-kA case, which agrees well with the estimation.

Figs. 6 and 7 show the measurement results for the triangular pulses. The AC loss shows the linear dependency on the ramp

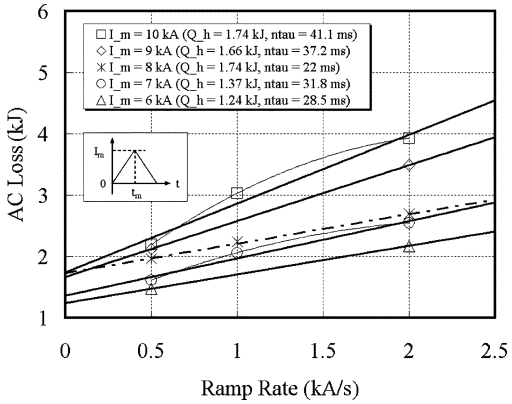

Fig. 6. Measured AC loss with the variation of the ramp rate of a single triangular pulse: Data was fit to straight lines to get the AC loss parameters and to curved lines to analyze the hysteresis loss in detail. In case of 8 kA, fit is expressed with a dotted line since it deviated from the normal trend.

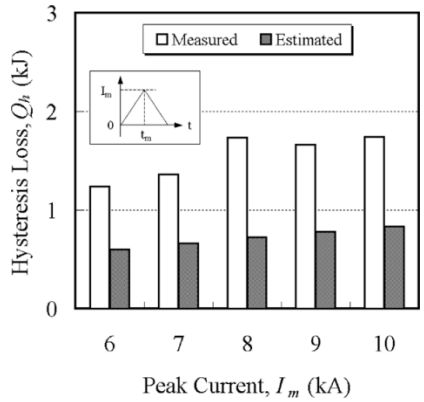

Fig. 7. Measured and estimated hysteresis loss in case of a single triangular pulse application.

rate with a certain deviation. As the peak current increases, the slope of the fitted line, which is proportional to $n\tau$, also increased monotonically except the 8-kA case. The increase of $n\tau$ could be explained from the relation between the coupling time constant (τ) and the effective transverse resistivity $(\rho_\perp)$ of the cable:

$$\tau = \frac{\mu_0 L_p^2}{8\pi^2 \rho_\perp}. \tag{8}$$

When the coil is charged, the cable is subjected to the Lorentz force in the transverse direction. If the force becomes larger than a certain level, the decrease in the contact resistance between strands becomes effective. As a result, the coupling current loss, or $n\tau$, is increasing. The maximum BI load throughout the channels is 0.9∼2.4 MPa at 6∼10 kA and the result can be related to the above explanation.

The measured hysteresis loss increases linearly with the peak current as expected. However, as shown in Fig. 7, the result is about 2 times larger than the estimation. Though there are many factors contributing to this result, the hysteresis loss of Incoloy 908 jacket could play a substantial role to this. The hysteresis loss of Incoloy 908 is 4.1 mJ/cc during ±1 T cycle at 4 K [12] and the volume ratio between Incoloy 908 and non-copper part in the CICC is ∼3.7. Then, the loss in Incoloy 908 corresponds to 10% of the loss in the non-copper part for 10-kA pulse where the maximum field is ∼2 T.

Note that if the measured data is fit to a curve as shown in Fig. 6, the error reduces considerably. In case of 10 kA, when the data is fit to the second-order polynomial, the value at the zero ramp rate, or the hysteresis loss, is 1.1 kJ. Since the estimated value is 0.83 kJ, the error falls to about 30%.

V. Conclusion

The AC losses of the KSTAR CSMC have been measured by a calorimetric method. In case of the DC-biased sinusoidal wave, the measured hysteresis loss agrees with the theoretical estimation within 15%. It is inferred that the coupling loss could be reduced from the cyclic load effect with the BI load more than 4 MPa.

The coupling loss increases linearly with the frequency of the sine wave and the ramp rate of the triangular wave. The $n\tau$ varies with the amplitude of field strength and $n\tau$ increases with the field amplitude within the range of 0.29∼4.3 T.

A further investigation about the $n\tau$ at a higher field region is required. However, within the range of our experiment, the $n\tau$ is confirmed to be lower value than the KSTAR design parameter 60 ms.

References

[1] H. Kim *et al.*, "Winding scheme for superconducting tokamak coils with cable-in-conduit conductor," *Fusion Eng. Des.*, vol. 55, no. 1, pp. 21–33, 2001.

[2] S. Baang *et al.*, "The background magnets of the Samsung superconductor test facility," *IEEE Trans. Appl. Supercond.*, vol. 11, pp. 2082–2085, 2001.

[3] S. Lee *et al.*, "Fabrication of cables for the background-field magnet system of SSTF," *IEEE Trans. Appl. Supercond.*, vol. 12, no. 1, pp. 583–585, 2002.

[4] B. S. Lim *et al.*, "Fabrication of the KSTAR Superconducting CICC," *IEEE Trans. Appl. Supercond.*, vol. 12, no. 1, pp. 591–594, 2002.

[5] Y. Takahashi *et al.*, "AC loss measurement of 46 kA-13 T Nb3Sn conductor for ITER," *IEEE Trans. Appl. Supercond.*, vol. 11, no. 1, pp. 1546–1549, 2001.

[6] C. Y. Gung, Ph.D Thesis, MIT, 1993.

[7] C. Y. Gung, M. Takayasu, and J. V. Minervini, "Experimental estimation of energy dissipation in ITER central solenoid superconductor," in *Proc. 15th IEEE/NPSS Symp.*, New York, 1994, pp. 692–695.

[8] A. Nijhuis *et al.*, "Electromagnetic and mechanical characterization of ITER CS-MC conductors affected by transverse cyclic loading, part 1: coupling current loss," *IEEE Trans. Appl. Supercond.*, vol. 9, no. 2, pp. 1069–1072, 1999.

[9] T. Ando *et al.*, "Pulsed operation test results of the ITER-CS model coil and CS insert," *IEEE Trans. Appl. Supercond.*, vol. 12, no. 1, pp. 496–499, 2002.

[10] P. Bruzzone, "Coupling currents loss in Nb3Sn cable-in-conduit conductors," *IEEE Trans. Appl. Supercond.*, vol. 12, no. 1, pp. 524–527, 2002.

[11] A. Nijhuis *et al.*, "Electromagnetic and mechanical characterization of ITER CS-MC conductors affected by transverse cyclic loading, Part 3: mechanical properties," *IEEE Trans. Appl. Supercond.*, vol. 9, no. 2, pp. 165–168, 1999.

[12] L. S. Toma, M. M. Steeves, and R. P. Reed, *Incoloy Alloy 908 Data Handbook*. : PFC, MIT, 1994.